Progress In Electromagnetics Research Letters, Vol. 111, 45–54, 2023

A Tri-Mode Hybrid Antenna for Quad-Band Applications

Wang Ren* **and Ping Yang**

Abstract—This paper presents a coplanar waveguide (CPW)-fed tri-mode hybrid antenna that is suitable for quad-band applications. The antenna design is compact, measuring only $30 \times 30\,\text{mm}^2$, and consists of a zeroth-order resonator (ZOR) antenna, a torch-shaped monopole antenna, and a T-shaped slot antenna. The most significant feature of this design is its ability to provide three independent working modes, making it a hybrid antenna. By incorporating a Composite Right/Left-Handed Transmission Line (CRLH-TL) unit cell, the first mode is excited as a ZOR antenna, corresponding to the lowest resonance at around 1.57 GHz. The second mode relies on the torch-shaped monopole antenna with two resonances at about 2.5 GHz and 3.5 GHz. The third mode employs the T-shaped slot antenna with a resonance at around 5.5 GHz. Experimental results demonstrate that the proposed antenna exhibits a wide and multi-band behavior with impedance bandwidths of 60 MHz (1.56–1.62 GHz), 210 MHz (2.30–2.51 GHz), 370 MHz (3.40–3.77 GHz), and 1100 MHz (5.05–6.15 GHz). This antenna can not only support the current GPS/WLAN/WiMAX systems but can also be considered as one element of a multiple-input-multiple-output (MIMO) antenna array for the fifth-generation (5G) mobile communication in the sub-6 GHz frequency range.

1. INTRODUCTION

The prevalence of smart portable devices in modern life has significantly improved people's well-being. However, this trend also poses new challenges and opportunities for antenna designers. On one hand, various wireless applications demand smaller antennas. Yet, conventional antennas are mainly limited by the resonating frequency in terms of size, which makes it challenging to miniaturize them, especially for low-frequency applications. On the other hand, effective data transfers require high-quality broadband and multiband antennas. Therefore, developing antennas that can simultaneously support multiple popular communication protocols while maintaining a small size is of great interest.

Metamaterials have been widely used in antenna design in recent years because of their unique resonance properties. One of the most prominent applications of metamaterials is the zeroth order resonator (ZOR) antenna, which exploits the ZOR phenomenon to achieve miniaturization and high performance [1–4]. ZOR phenomenon occurs when a composite right/left-handed transmission line (CRLH-TL) is balanced, resulting in an infinite wavelength and a resonance frequency that is independent of the physical size of the antenna. ZOR antennas have attracted considerable attention from researchers in the field of antenna engineering, as they offer advantages such as very compact size, omnidirectional radiation pattern, low profile, and high gain [5–9]. ZOR antennas have also been applied to various domains, such as sub-6 GHz fifth-generation (5G) communication, wireless power transfer (WPT), radio frequency identification (RFID), and controlled reception pattern antenna (CRPA). However, there are still some challenges and limitations that need to be addressed, such as fabrication complexity, mutual coupling, radiation efficiency, and especially narrow bandwidth. Narrow bandwidth restricts the ability of ZOR antennas to satisfy the communication needs of modern

Received 26 April 2023, Accepted 12 June 2023, Scheduled 21 June 2023
* Corresponding author: Wang Ren (renwang@zjgsu.edu.cn).
The authors are with the School of Information and Electronic Engineering, Zhejiang Gongshang University, Hangzhou, China.

multifunctional smart devices. To achieve a wider bandwidth, two methods have been adopted in recent literature [10–19]. The first method is to lower the Q-factor of the ZOR by changing the distributed element values [10–15]. The second method is to excite another working mode of the ZOR antenna, such as the first negative order resonance (FNOR) mode, the first positive order resonance (FPOR) mode, and then combine them to yield a wider bandwidth [16–19]. Although these methods have widened the bandwidth of ZOR antenna to some degree, the improvement is relatively limited. To the best of our knowledge, very few tri-band or quad-band ZOR antennas have been reported in the open literature.

This paper presents a new CPW-fed tri-mode hybrid antenna that combines three kinds of antennas into one with four operating bands, aiming to enhance the bandwidth of ZOR antenna. The proposed hybrid antenna uses ZOR antenna mode for the lowest frequency band, enabling size shrinkage and overcoming the physical dimension limitations. Moreover, the combination of monopole antenna mode and slot antenna mode addresses the inherent narrow-band problem of ZOR mode. Experimental results show that the proposed quad-band hybrid antenna not only supports current GPS/WLAN/WiMAX systems but also serves as an element of MIMO antenna array for 5G mobile communication in the sub-6 GHz frequency range, with a small size of $30 \times 30\,\text{mm}^2$. Furthermore, the paper introduces a new multiband antenna design approach where different components inspire multiple resonance bands that have little impact on each other, facilitating the adjustment of specific resonances and reducing the antenna development cycle.

2. ANTENNA DESIGN

2.1. Design Evolution

To achieve an extended bandwidth, a three-step design evolution with three working modes has been adopted, as shown in Figure 1, denoted as Ant_A, Ant_B, and Ant_C (the proposed antenna). These antennas are printed directly on an FR4 substrate ($\epsilon_r = 4.3$, $\tan\delta = 0.025$) with dimensions of 30 mm × 30 mm × 1.6 mm, chosen for its cost-effectiveness and suitability for miniaturization. The simulated S-parameters, generated using CST Microwave Studio, are plotted in Figure 2.

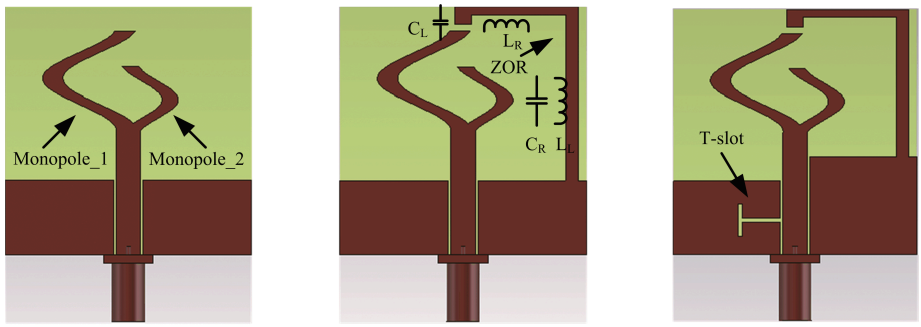

Figure 1. Design evolution of the proposed antenna: (a) Ant_A, (b) Ant_B, and (c) Ant_C.

In the first step, Ant_A, a CPW-fed torch-shaped dual-band monopole antenna was designed as the initial model. It consists of a microstrip feedline, two cosine-shaped radiating branches, and a co-planar ground plane on the top side of the substrate. As shown in Figure 2, the dual-band monopole antenna working mode successfully excites two resonances at around 2.5 GHz and 3.5 GHz.

In the second step, Ant_B uses a CRLH-TL unit cell to excite a ZOR antenna mode operating at approximately 1.6 GHz. The C_L, C_R, L_L, and L_R components of the CRLH-TL cell can be generated using a gap between two strips or a metal meandered stub. The simulated S-parameters shown in Figure 2 demonstrate that two different antenna modes (monopole antenna mode and ZOR antenna mode) have been successfully generated with resonances at approximately 1.6 GHz, 2.5 GHz, and 3.5 GHz.

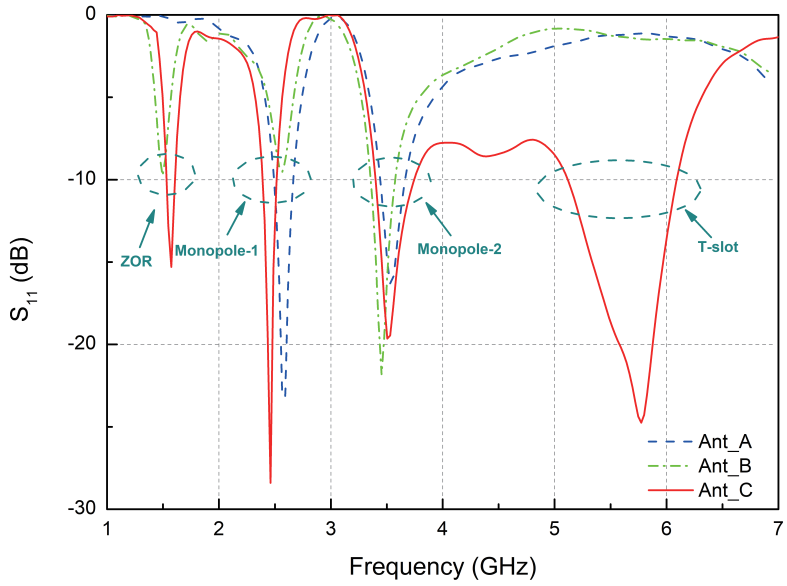

Figure 2. Simulated S_{11} of Ant_A, Ant_B, and Ant_C.

Finally, Ant_C further expands the antenna bandwidth by cutting a T-shaped slot in the ground plane, creating a slot antenna that excites an additional wide frequency band at 5.5 GHz. As shown in Figure 2, the proposed tri-mode hybrid antenna has broad operating bandwidths of 80 MHz (1.53–1.61 GHz), 120 MHz (2.39–2.51 GHz), 350 MHz (3.40–3.75 GHz), and 980 MHz (5.12–6.10 GHz), fully covering GPS, 2.4/5.2/5.8-GHz WLAN, and 3.5/5.5-GHz WiMAX applications. It can also be used in the fifth-generation mobile communication in the sub-6 GHz frequency range.

2.2. Antenna Geometry and Current Distribution

Figure 3 shows the configuration of the proposed CPW-fed tri-mode hybrid antenna, including its geometrical parameters. The antenna comprises three main components: a torch-shaped monopole, a CRLH-TL unit cell, and a slotted CPW ground plane. The torch-shaped monopole consists of two

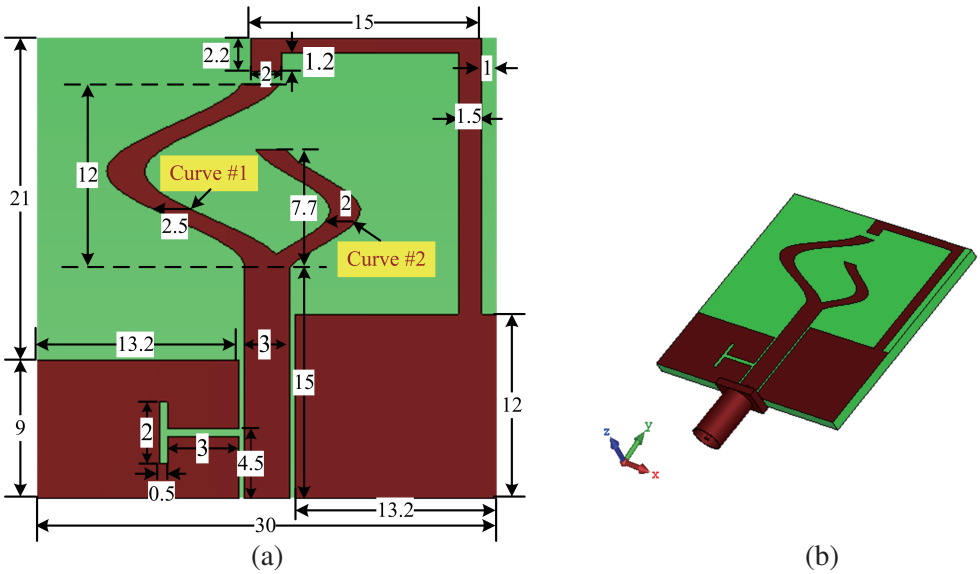

Figure 3. Geometry of the proposed antenna, (a): Top view, (b): 3-D view. (unit: mm).

cosine-shaped radiating branches, each obtained by translating a cosine curve along the X-axis for a certain distance. The widths of the cosine-shaped branches are indicated in Figure 3, with the lower-left corner serving as the coordinate origin. Equations (1) and (2) express the geometrical parameters of the two curves.

$$Left\_Curve: \begin{cases} x(t) = 4.5\cos(0.5t) + 11.5 \\ y(t) = t + 15 \end{cases} \quad t \in [0, 12] \tag{1}$$

$$Right\_Curve: \begin{cases} x(t) = 18.5 - 2.5\sin(0.7t) \\ y(t) = t + 12 \end{cases} \quad t \in [3, 10.7] \tag{2}$$

Figure 4 shows the surface current distribution analysis of the proposed quad-band antenna at 1.6 GHz, 2.5 GHz, 3.5 GHz, and 5.5 GHz. At 1.6 GHz, the surface current distribution mainly concentrates on the CRLH-TL unit cell, indicating that the lowest resonance is primarily controlled by this component, as shown in Figure 4(a). At 2.5 GHz and 3.5 GHz, the surface current distributions in Figures 4(b) and (c) mainly concentrate on the two branches of the torch-shaped monopole antenna, indicating that the two middle resonances are excited by the monopole antenna mode. At 5.5 GHz, the surface current distribution shown in Figure 4(d) mainly distributes around the T-shaped slot, indicating that the highest band is mainly determined by the slot antenna mode. Therefore, the proposed hybrid antenna utilizes different components to inspire multiple resonance bands, making it feasible to adjust individual resonant frequencies without making significant changes to the overall antenna design. This simplifies the antenna design process and shortens the design cycle.

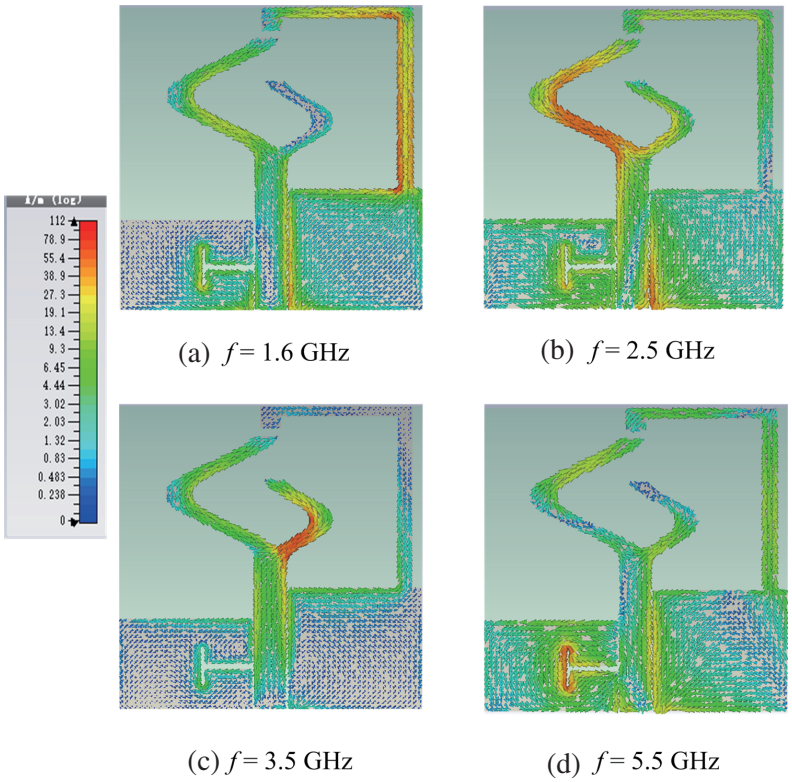

Figure 4. Simulated current distributions of the proposed antenna at (a) 1.6 GHz, (b) 2.5 GHz, (c) 3.5 GHz, and (d) 5.5 GHz.

2.3. Equivalent Circuit Model

To better comprehend the resonance behavior of the proposed antenna and provide a circuit-level simulation model, an effective equivalent circuit is extracted and analyzed. Due to the existence of

multiple resonances across a large band, a distributed equivalent circuit model is established, which comprises three parts corresponding to the ZOR antenna mode, dual-band monopole antenna mode, and slot antenna mode, as shown in Figure 5. The circuit model of the ZOR antenna is a combination of a capacitance $C1$ in series with an inductance $L1$ and a shunt capacitance $C2$ in parallel with an inductance $L2$. The monopole antenna and slot antenna are equivalent to series RLC circuits. The final circuit parameters for the proposed hybrid antenna are optimized by advanced design system (ADS) and listed in Table 1.

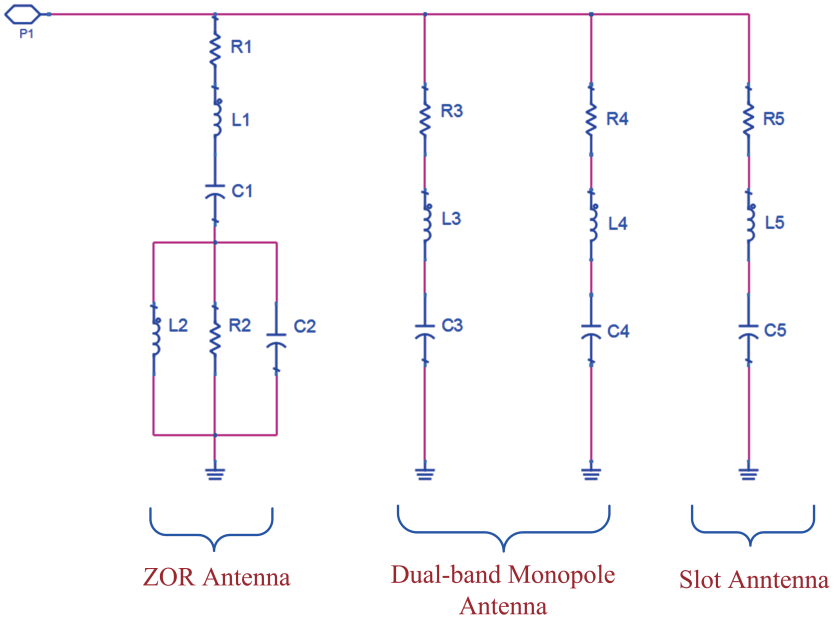

Figure 5. Equivalent circuit model of the proposed antenna.

Table 1. Optimal equivalent circuit parameters.

Parameter	Value	Parameter	Value	Parameter	Value
$R1$	0.2 ohm	$L1$	30.5 nH	$C1$	0.34 pF
$R2$	36.2 ohm	$L2$	15.7 nH	$C2$	0.34 pF
$R3$	56.0 ohm	$L3$	20.5 nH	$C3$	0.22 pF
$R4$	45.0 ohm	$L4$	10.0 nH	$C4$	0.20 pF
$R5$	55.0 ohm	$L5$	4.5 nH	$C5$	0.16 pF

3. SIMULATION AND MEASURED RESULTS

Figure 6 shows a photograph of the CPW-fed tri-mode hybrid antenna that was fabricated. The S-parameters of the prototype were measured using an Agilent E5071C Vector Network Analyzer. The radiation patterns were measured in an anechoic chamber at Ningbo University. Figure 7 shows a comparison of the reflection coefficients simulated by computer simulation technology (CST), ADS, and the measured results. As depicted in the figure, the proposed antenna successfully excited four distinct bands at 1.6 GHz, 2.5 GHz, 3.5 GHz, and 5.5 GHz, each by different parts of the antenna. The proposed antenna's -10 dB impedance bandwidths were measured to be 60 MHz (1.56–1.62 GHz), 210 MHz (2.30–2.51 GHz), 377 MHz (3.40–3.77 GHz), and 1100 MHz (5.05–6.15 GHz), meeting the requirements of various communi-cation standards, including 1.575-GHz GPS, 2.4/5.2/5.8-GHz WLAN,

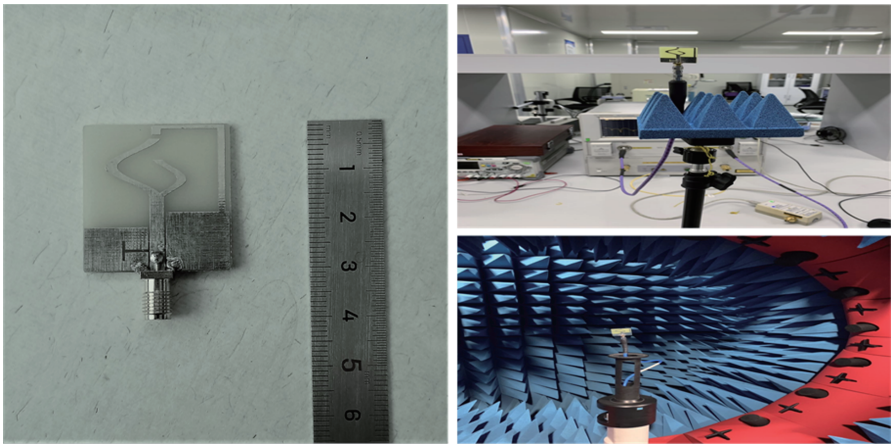

Figure 6. A photograph of the fabricated proposed antenna and the test environment.

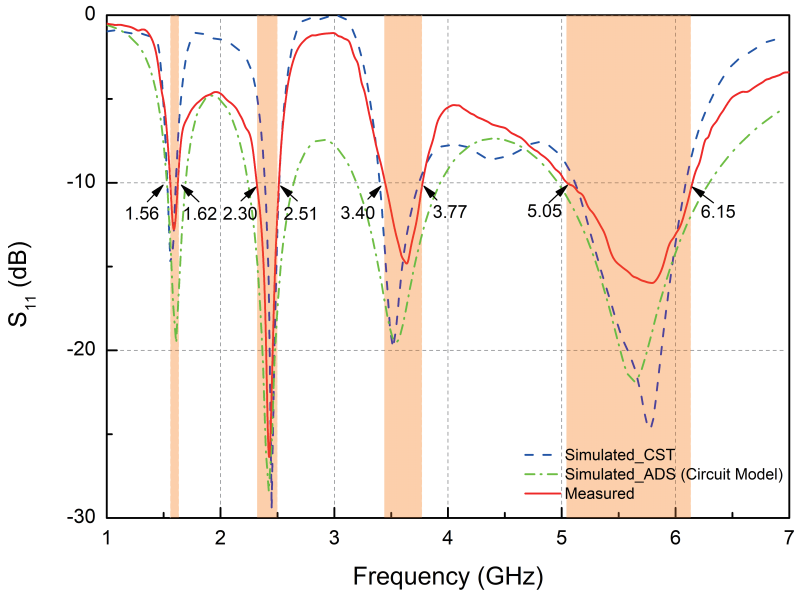

Figure 7. Simulated and measured S_{11} of the proposed antenna. It can cover the 1.575-GHz GPS, 2.4/5.2/5.8-GHz WLAN, 3.5/5.5-GHz Wi-MAX, and part of the sub-6G band in 5G mobile communication.

3.5/5.5-GHz Wi-MAX, and part of the sub-6G band in 5G mobile communication. The offsets of the center frequencies between simulation and testing are 20 MHz, 45 MHz, 10 MHz, and 10 MHz in the GPS frequency band, 2.4 GHz frequency band, 3.5 GHz frequency band, and 5.5 GHz frequency band, respectively. The results from the simulation and testing exhibit good consistency.

Figure 8 shows the simulated and measured far-field radiation patterns in the xz- and yz-planes at 1.6 GHz, 2.5 GHz, 3.5 GHz, and 5.5 GHz. The proposed antenna exhibits good omnidirectional radiation patterns in the xz-plane and nearly bi-directional radiation patterns in the yz-plane. As all the radiating elements, including the CRLH-TL unit, torch-shaped monopole, and T-shaped slot, contain both vertical and horizontal components, a certain amount of cross-polarization is observed. Generally, antennas with low polarization purity may affect the quality and reliability of communication. However, in some indoor environments such as high-rise buildings, underground parking lots, and subway tunnels, where signal propagation is obstructed and reflected, using antennas with lower polarization purity may actually

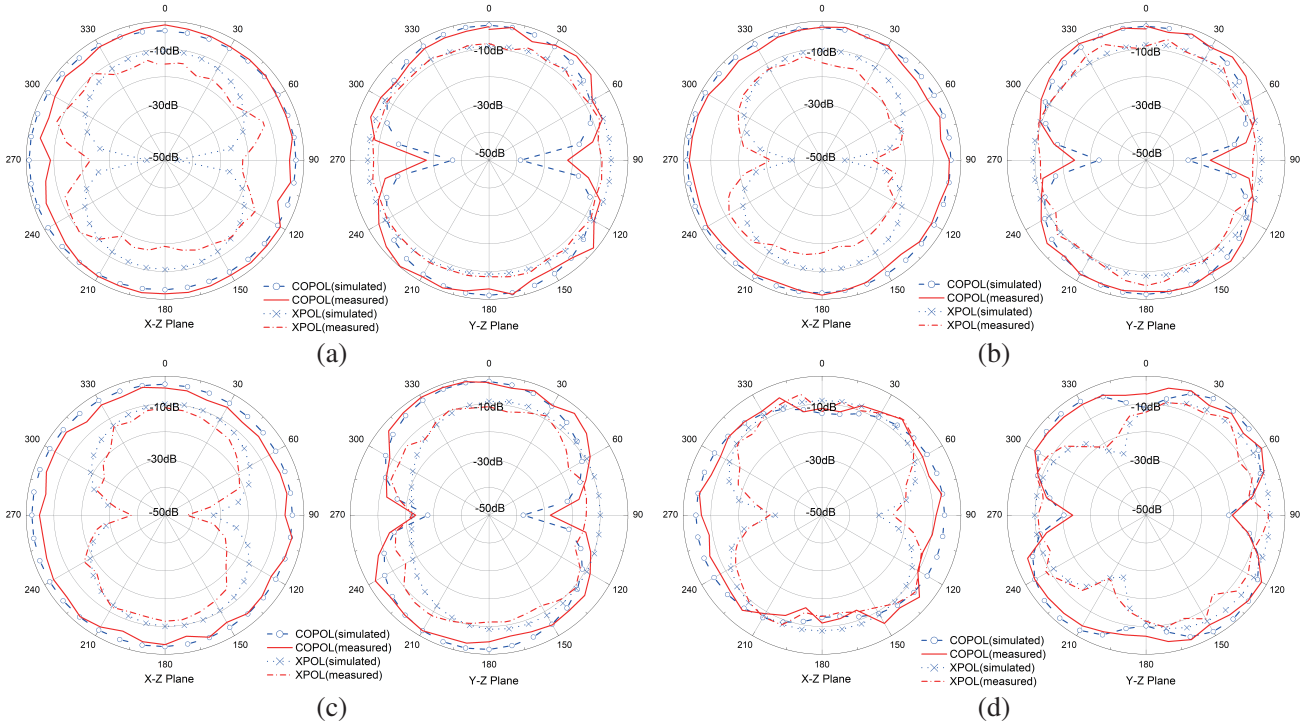

Figure 8. Simulated and measured radiation patterns of the proposed antenna at (a) 1.6 GHz, (b) 2.5 GHz, (c) 3.5 GHz, and (d) 5.5 GHz.

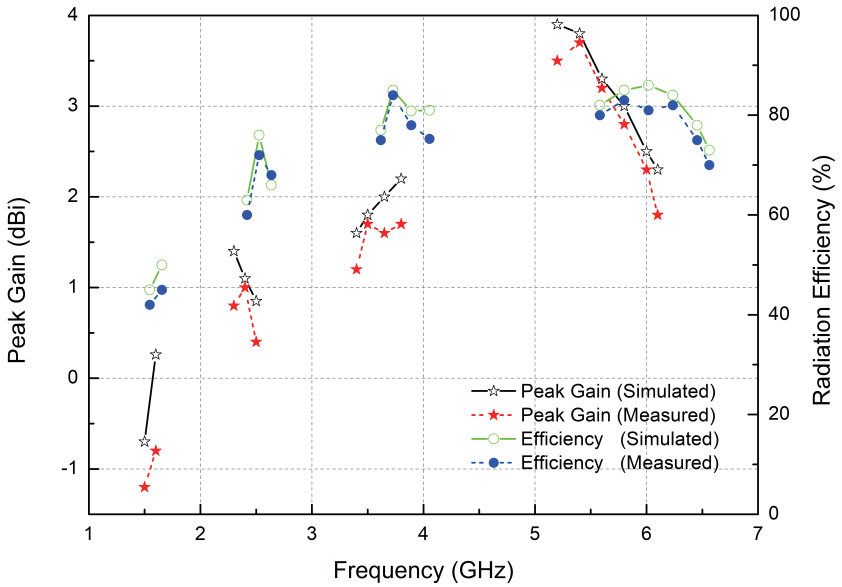

Figure 9. Gains and efficiencies of the proposed antenna. The measured peak gains in the four working bands are −0.8 dBi, 1.0 dBi, 1.7 dBi, and 3.7 dBi. The measured radiation efficiencies are 45%, 72%, 84%, and 81% at 1.6 GHz, 2.5 GHz, 3.5 GHz, and 5.5 GHz, respectively.

achieve better performance and coverage. For example, in some commercial multi-band antenna design cases (such as Taoglas PA.700 Viking series), due to the low polarization purity, high gains can be achieved on both horizontal and vertical polarization planes. This feature is very useful in certain wireless communications where the antenna orientation is not fixed, and the reflections or multipath

Table 2. Performance comparison with other multiband antennas.

Ref	Total size (λ_0)	Frequency range (GHz)	Bandwidth (MHz)	Peak gain (dBi)
[4]	0.21×0.21	2.37–2.41/5.5–5.9	40/400	1.75/1.73
[13]	0.74×0.42	4.8–5.2/5.8–5.84/6.3–6.34	400/40/40	1/0.8/0.6
[15]	0.67×0.67	2.48–2.5/3.4–3.5	20/100	4.0/4.3
[18]	0.25×0.19	1.8-3.75	1950	2.77
[20]	0.29×0.23	1.575–1.665/2.4–2.545/ 3.27–3.97/5.17–5.93	90/145/700/760	3.55/3.93/5.02/4.86
[21]	0.30×0.27	1.515–1.625/2.33–2.49/ 3.42–3.70/5.05–5.94	110/160/280/890	−1.0/3.2/2.3/4.5
This work	0.16×0.16	1.56–1.62/2.30–2.51/ 3.40–3.77/5.05-6.15	60/210/370/1100	−0.8/1.0/1.7/3.7

Table 3. Size comparison with several commercial GPS antennas.

Trimble		NovAtel		Garmin	
Product Series	Size	Product Series	Size	Product Series	Size
$Bullet^{TM}$	Diameter: 43 mm Height: 84 mm	GPS-702	Length: 45 mm Width: 44 mm Height: 13.2 mm	GA-26	Diameter:35 mm Height:8 mm
R8s	Diameter: 130 mm Height: 125 mm	GPS-703	Length:38 mm Width:38 mm Height: 12.7 mm	GA-37	Diameter: 61 mm Height: 18 mm
$Tornado^{TM}$	Diameter: 190 mm Height: 67 mm	GPS-704	Length: 50 mm Width:50 mm Height: 15.5 mm	GA-38	Diameter: 61 mm Height: 33 mm

signals may be present from any plane.

Figure 9 displays the gains and radiation efficiencies of the proposed antenna for GPS/WLAN/WiMAX bands. The measured peak gains in the four working bands are −0.8 dBi, 1.0 dBi, 1.7 dBi, and 3.7 dBi. The measured radiation efficiencies are 45%, 72%, 84%, and 81% at 1.6 GHz, 2.5 GHz, 3.5 GHz, and 5.5 GHz, respectively. The lower efficiency at 1.6 GHz is mainly due to the conductor losses caused by the ZOR structure and a relatively large dielectric loss of FR4 substrate. If antenna efficiency is a more critical concern, a low-loss material with a similar dielectric constant, such as AD450, can be used as an alternative. This change would result in approximately 10% efficiency improvement while keeping the working bandwidth almost unchanged.

Table 2 is presented to evaluate the proposed antenna, with a performance comparison to recently reported multiband antenna designs. λ_0 represents the lowest resonant frequency of the antenna. Compared with ZOR antennas [4, 13, 15, 18] utilizing CRLH units, the proposed design demonstrates significant advantages in both operation bands and antenna size. Furthermore, a comparison with other multiband antennas that do not employ CRLH units [20, 21] is also provided for a more comprehensive evaluation. The proposed antenna shows excellent quad-band resonances in a smaller size, thanks to the CRLH unit, which is advantageous for antenna miniaturization and integration requirements. Therefore, the proposed antenna can be regarded as a competitive candidate for various multifunctional wireless applications. In order to better illustrate the advantages of our design in miniaturization and considering that the size of a multi-frequency antenna is generally determined by its lowest resonant frequency, we also compare the dimensions of 9 mainstream products from three professional GPS

antenna manufacturers: Trimble, NovAtel, and Garmin, as shown in Table 3. It can be seen that from the perspective of miniaturization, our design has already possessed good product competitiveness.

4. CONCLUSIONS

This paper presents a compact tri-mode hybrid antenna for quad-band applications. The proposed antenna demonstrates the ability to individually excite three operating modes, including ZOR antenna mode, dual-band monopole antenna mode, and slot antenna mode, with a relatively compact size of $30 \times 30\,\text{mm}^2$. Both the simulated and measured results show that the proposed antenna is capable of fully satisfying the requirements of the 1.575-GHz GPS (1.57–1.59 GHz), 2.4/5.2/5.8-GHz WLAN (2.4–2.485, 5.15–5.35, and 5.725–5.825 GHz), and 3.5/5.5-GHz WiMAX (3.40–3.60, and 5.25–5.85 GHz) applications. Furthermore, it can also be used as one element of MIMO antenna array for the 5G mobile communication system. The simulated and measured results demonstrate the effectiveness of the proposed antenna for various multifunctional wireless applications.

ACKNOWLEDGMENT

This research was supported by the Public Welfare Research Project and Natural Science Foundation of Zhejiang Province, grant number LGG19F010005.

REFERENCES

1. Caloz, C. and T. Itoh, *Electromagnetic Metamaterials: Transmission Line Theory and Microwave Applications*, Wiley, New York, 2004.
2. Ooi, S. Y., P. S. Chee, and E. H. Lim, "A zeroth-order slot-loaded cap-shaped patch antenna with omnidirectional radiation characteristic for UHF RFID tag design," *IEEE Trans. Antennas Propag.*, Vol. 71, No. 1, 131–139, 2023.
3. Nguyen, M. A. and G. Bien, "Design of an out-folded patch antenna with a zeroth-order resonance for non-invasive continuous glucose monitoring," *IEEE Trans. Antennas Propag.*, Vol. 70, No. 10, 8932–8940, 2022.
4. Li, Z. Y., Y. Z. Zhu, H. L. Yang, G. H. Peng, and X. Y. Liu, "A dual-band omnidirectional circular polarized antenna using composite right/left-handed transmission line with rectangular slits for unmanned aerial vehicle applications," *IEEE Access*, Vol. 8, 100586–100595, 2020.
5. Lai, A., T. Itoh, and C. Caloz, "Composite right/lefted-handed transmission line metamaterials," *IEEE Microw. Mag.*, Vol. 5, No. 3, 34–50, 2004.
6. Dong, Y. and T. Itoh, "Metamaterial-based antenna," *Proceedings of the IEEE*, Vol. 100, No. 7, 2271–2285, 2012.
7. Mohammad, A. and C. Raghvendra, "Metamaterial circularly polarized antennas: Integrating an epsilon negative transmission line and single split ring-type resonator," *IEEE Antenna Propag. Mag.*, Vol. 63, No. 4, 60–77, 2021.
8. Luo, Y., Y. M. He, S. G. Xu, and G. L. Yang, "Programmable zeroth-order resonance with uniform manipulation using the nonlinearity of PIN diodes," *IEEE Antennas Wireless Propag. Lett.*, Vol. 18, No. 11, 2419–2423, 2019.
9. Wang, Z., S. N. Zhao, and Y. D. Dong, "Pattern reconfigurable, low-profile, vertically polarized, ZOR-metasurface antenna for 5G application," *IEEE Trans. Antennas Propag.*, Vol. 70, No. 8, 6581–6591, 2022.
10. Chi, P. L. and Y. S. Shih, "Compact and bandwidth-enhanced zeroth-order resonant antenna," *IEEE Antennas Wireless Propag. Lett.*, Vol. 14, 285–288, 2015.
11. Harish, A. M., B. R. Gudibandi, and K. D. Sriram, "Triple-band zeroth-order epsilon-negative antenna using two pseudo-open termination unit cells for C-band applications," *IEEE Antennas Wireless Propag. Lett.*, Vol. 18, No. 5, 1011–1015, 2019.

12. Luo, X. S., Z. B. Weng, and L. Yang, "A circularly-polarized antenna with broadband based on CRLH-TL for navigation applications," *Proceedings of 6th Asia-Pacific Conference on Antenna and Propagation*, Xi'an, China, 2017.
13. Lbrahim, A. A., M. A. Abdalla, and Z. R. Hu, "Compact ACS-fed CRLH MIMO antenna for wireless applications," *IET Microw. Antennas Propag.*, Vol. 12, No. 6, 1021–1025, 2018.
14. Saeid. K. and R. Vahid, "A novel ZOR antenna with a capablility to change polarization and diversity," *Progress In Electromagnetics Research Letters*, Vol. 93, 73–80, 2020.
15. Zhang, J. H., S. Yan, and G. A. E. Vandenbosch, "Realization of dual band pattern diversity with a CRLH-TL inspired reconfiguration metamaterial," *IEEE Trans. Antennas Propag.*, Vol. 66, No. 10, 5130–5138, 2018.
16. Ning, Y. W., Y. Fan, and Y. D. Dong, "Omnidirectional circularly polarized antenna based on dual zeroth-order resonances," *Proceeding of 2019 IEEE Asia-Pacific Microwave Conference (APMC)*, Singapore, 816–818, 2019.
17. Liu, L. Y. and B. Z. Wang, "Compact circularly polarized ZOR and FOR antenna employing CRLH transmission lines," *Microwave Opt. Technol. Lett.*, Vol. 58, No. 4, 964–969, 2016.
18. Shi, Y., Q. S. Zeng, Z. F. Wang, Q. Q. Si, Y. D. Zhang, T. Qiu, Y. Q. Shang, and Y. Wu, "Wideband asymmetric coplanar waveguide antenna using composite right/left-handed transmission line," *Microwave Opt. Technol. Lett.*, Vol. 64, No. 6, 1062–1069, 2022.
19. Pratap, L. B., A. Mohan, and D. Arijit, "Compact bandwidth-extended CRLH-TL based monopole antenna," *Proceedings of IEEE International Symposium on Antennas and Propagation and USNC-URSI Radio Science)*, Denver, USA, 2022.
20. Cao, Y. F., S. W. Cheung, and T. I. Yuk, "A multiband slot antenna for GPS/WiMAX/WLAN systems," *IEEE Trans. Antennas Propag.*, Vol. 63, No. 3, 952–958, 2015.
21. Sun, X., G. Zeng, H. C. Yang, X. J. Liao, and L. Wang, "Design of an edge-fed quad-band slot antenna for GPS/WiMAX/WLAN applications," *Progress In Electromagnetics Research Letters*, Vol. 28, 111–120, 2012.